SINTEF
PROCEEDINGS 5

International Conference Organised by IBPSA-Nordic, 13th–14th October 2020, OsloMet

BuildSIM-Nordic 2020

Selected papers

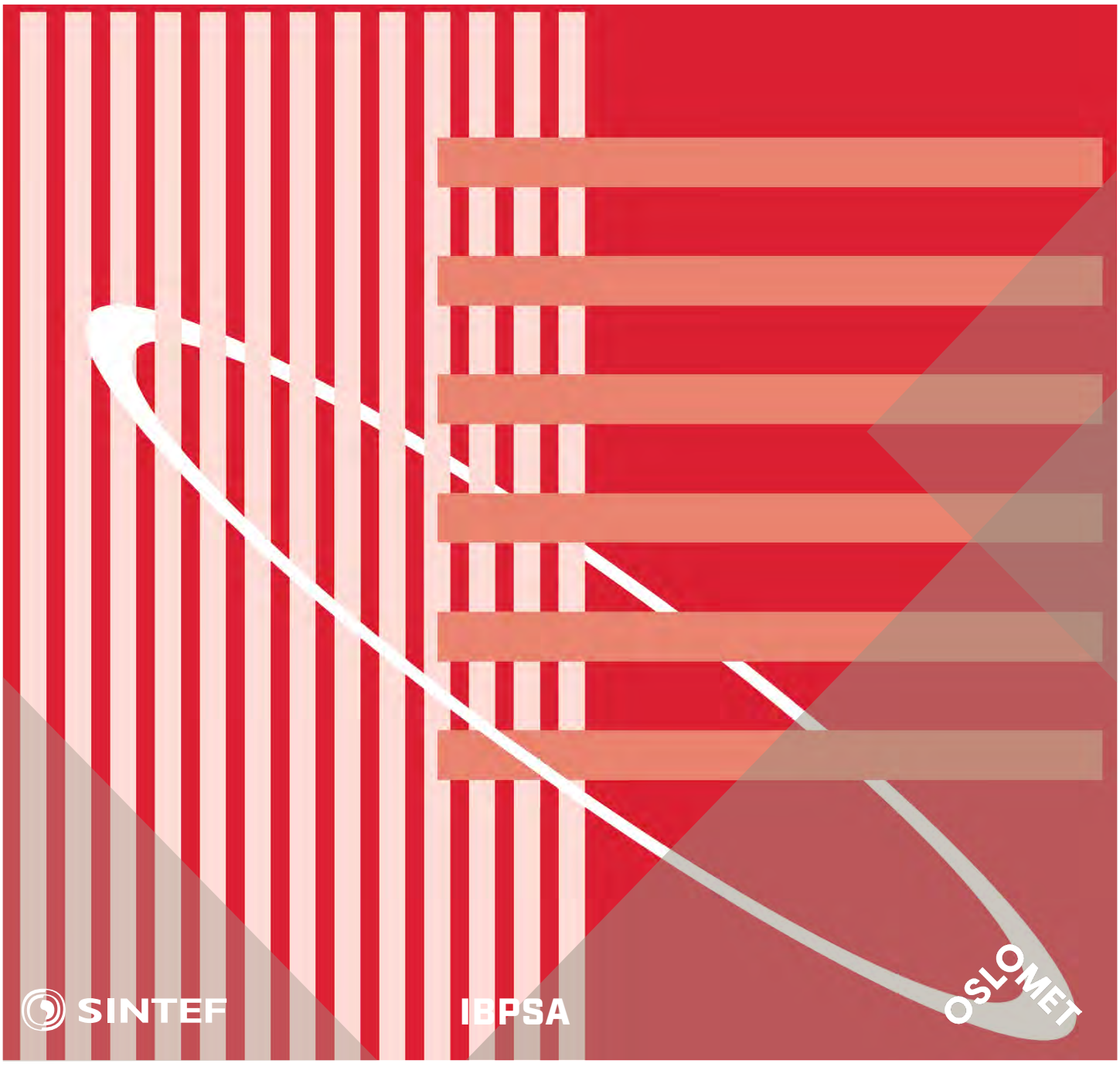

SINTEF Proceedings

Editors:
Laurent Georges, Matthias Haase, Vojislav Novakovic and Peter G. Schild

BuildSIM-Nordic 2020

Selected papers

International Conference Organised by IBPSA-Nordic,
13th–14th October 2020, OsloMet

SINTEF Academic Press

SINTEF Proceedings no 5
Editors:
Laurent Georges, Matthias Haase, Vojislav Novakovic and Peter G. Schild
BuildSIM-Nordic 2020
Selected papers
International Conference Organised by IBPSA-Nordic,
13th–14th October 2020, OsloMet

Keywords:
Building acoustics, Building Information Modelling (BIM), Building physics, CFD and air flow, Commissioning and control, Daylighting and lighting, Developments in simulation, Education in building performance simulation, Energy storage, Heating, Ventilation and Air Conditioning (HVAC), Human behavior in simulation, Indoor Environmental Quality (IEQ), New software developments, Optimization, Simulation at urban scale, Simulation to support regulations, Simulation vs reality, Solar energy systems, Validation, calibration and uncertainty, Weather data & Climate adaptation, Fenestration (windows & shading), Zero Energy Buildings (ZEB), Emissions and Life Cycle Analysis

Cover illustration: IBPSA-logo

ISSN 2387-4295 (online)
ISBN 978-82-536-1679-7 (pdf)

SINTEF Academic Press
Address: Børrestuveien 3
PO Box 124 Blindern
N-0314 OSLO
Tel: +47 40 00 51 00

www.sintef.no/community
www.sintefbok.no

Analysis of the interfacial mixing in the gravity-driven counterflow through a large vertical opening using Large Eddy Simulation

Elyas Larkermani [1*], Laurent Georges [1]
[1] Department of Energy and Process Engineering, Norwegian University of Science and Technology, NTNU, Trondheim, Norway
* *corresponding author: elyas.larkermani@ntnu.no*

Abstract

The study of natural convection flows in multizone enclosures is a topic of great importance due to its direct influence on room air circulation patterns, distribution of indoor air contaminants, and thermal comfort inside buildings. In this research, ANSYS Fluent is used to investigate the density-driven bidirectional flow through a large vertical opening connecting two isothermal reservoirs, the so-called bulk flow regime. Many research works on the natural convection flow through a large vertical opening between two enclosures have been done. However, they paid less attention to the unsteady flow structures generated by the sophisticated bidirectional flow, especially in the middle of the doorway. Large Eddy Simulation (LES) results show the development of unsteady flow structures in the middle of the doorway, a phenomenon called "interfacial mixing". This phenomenon has been hardly documented in the literature, only using experiments. Even though unsteady flow structures develop, they do not significantly affect bulk quantities such as the discharge coefficient (C_d).

Introduction

The behavior of natural convection in confined spaces has attracted a lot of attention originating from its application in buildings air conditioning, contaminant spread and electronic equipment cooling. The vast majority of these spaces include internal partitions that the flow can traverse partially. In most situations, the presence of internal partitions with an opening lead to an intrinsically three-dimensional and transient flow field. The characteristics of such complicated flow are of strong interest to many communities and researchers. Several parameters can have an important role in driving this flow such as temperature differences, door motion, occupant motion or wind dynamic pressure. In past investigations, Computational Fluid Dynamics (CFD) simulations of the natural convection flow through a large vertical opening between two enclosures have been performed, but mostly using RANS, and/or two-dimensional assumption, and/or what can be considered today as very coarse grids. This made the unsteady flow structures impossible to be captured by these CFD simulations. From the experimental side, several past studies reported on the flows in differently heated enclosures separated by a partition wall. While these studies analyzed the flow inside these enclosures, the flow within the doorway itself was measured for a limited number of locations. However, the CFD standards of today enable to better investigate the unsteady nature of the bidirectional flow inside large vertical openings.

Two separate mechanisms for natural convection flow between a hot and a cold zone were investigated in the experimental study of Scott et al. [1]: the *boundary layer* regime and the *bulk density-driven* regime. The transition between both regimes was established as a function of the aperture size located in the middle of the partition wall. In another similar work, the effect of internal partitions on the convective heat transfer across an enclosure was described by Neymark et al. [2]. They developed a Nusselt-Rayleigh correlation using the aperture width and a resistance model. Georges et al. [3] conducted RANS simulations using the RNG $k-\varepsilon$ model and ANSYS Fluent for two rooms with an open door in the partition wall. They proved that the thermal radiation could affect the transition between the two aforementioned regimes and opposed to previous reports claiming that the aperture size was the main driving parameter causing such transition.

Favarolo and Manz [4] employed the LVEL $k-\varepsilon$ turbulence model [5] in the FLOVENT commercial CFD software to analyze the influence of different parameters such as temperature difference between indoor and outdoor air on the airflow rate through a large open window. The vertical position and the horizontal distance of the opening from the wall were diagnosed to have the greatest and minor impact on the discharge coefficient (C_d), respectively. Based on their literature review, the value of C_d varies between 0.3 and 0.8, and the origin of these large variations is not clear to the authors. Allard and Utsumi [6] mentioned that this phenomenological coefficient takes into consideration the contraction of the flow while it passes through the opening. They concluded that the definition of C_d is still ambiguous and requires more precision. Pelletret et al. [7] investigate various approaches to determine the C_d as a function of opening height or temperature difference. They also show the difficulty in determining the C_d and point out that a variety of definitions for this coefficient has been introduced in the literature. Hence, despite the significant amount of numerical and experimental studies conducted to date, no clear conclusion can be drawn from previous studies.

The standard model to evaluate the airflow in a doorway, extensively used in building performance simulation (BPS), assumes two isothermal reservoirs and a one-dimensional inviscid steady-state flow. Both assumptions lead to a simple model based on the Bernoulli equation which is defined here as the theoretical model [8]. The resulting theoretical flow is then corrected using the C_d to match the actual airflow in the doorway. Uncertainties related to this modeling framework remain unknown. In particular, the effect of the unsteady flow regime on the value of the discharge coefficient needs to be elucidated.

When both reservoirs are isothermal and the room air temperature is in thermal equilibrium with the wall temperature surrounding it, the airflow in the doorway is in the bulk flow regime. The air temperature difference (ΔT) between both zones and the aperture geometry are the only physical parameters needed to define the flow. The temperature difference between the two zones leads to different bulk air densities and, consequently, different hydrostatic pressure fields. Due to the conservation of mass, both hydrostatic pressure fields are equal at the neutral plane (NP) located near the middle of the doorway. The difference of hydrostatic pressure above and below the NP generates a counterflowing stream of warm and cold air. A schematic of the velocity profile of this bidirectional flow in the vertical centerline of the doorway is shown in Fig. 1. Assuming an inviscid flow, the velocity profile shows a sharp gradient at the level of the NP (i.e. dashed lines in Fig. 1). With a viscous flow, three related phenomena can occur. Firstly, the two airstreams going in opposite directions create a shear layer. Secondly, Wilson and Kiel [9] reported some interfacial mixing due to re-entrainment effects. According to these authors, the resulting velocity and temperature profiles show a smoother transition at the level of the neutral plane (i.e. solid line in Fig. 1). Thirdly, a similar study by Lefauve et al. [10] using two reservoirs connected by a long channel demonstrated that a sustained stratified shear flow could generate large unsteady flow structures. Consequently, the mass and heat flows exchanged through the doorway will be reduced compared to the inviscid flow (i.e., the assumption used in the standard model).

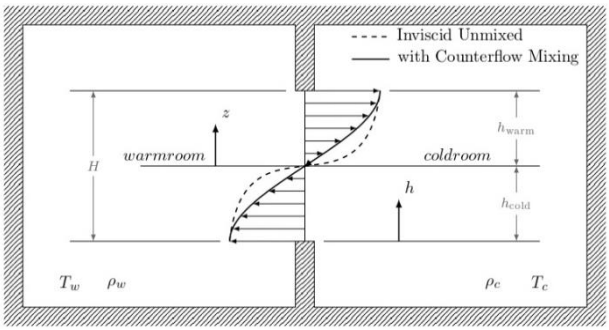

Figure 1: Inviscid and actual profiles of the streamwise velocity for the bidirectional flow in a doorway.

The present work investigates viscous effects and the resulting unsteady flow in the middle of the doorway using Large Eddy Simulation (LES). Two large reservoirs are created by connecting two large isothermal volumes of equal size by a vertical solid partition. The single rectangular aperture located in the middle of the vertical partition enables the air to flow between the two zones. The primary objective of the present study is the interfacial mixing, meaning to characterize the mixing process (i.e. shear, re-entrainment and unsteady flow structures) and its influence on the volume airflow rate and heat transfer across the opening.

Numerical Method

Multizone enclosure description

The bidirectional airflow is generated at the aperture of height $h = 2m$ and width $w = 1m$. Each zone has the same length $L_0 = 16m$ in all spatial directions and is filled with air with constant thermodynamic properties. Figure 2 illustrates the geometry of the three-dimensional multizone enclosure.

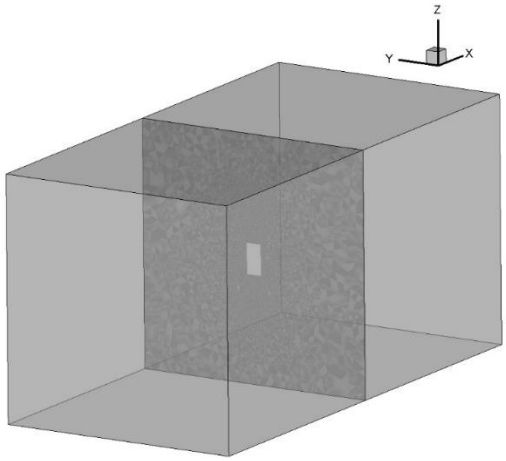

Figure 2: Three-dimensional multizone enclosure configuration.

Governing equations

After applying an implicit filtering operator and considering the Boussinesq approximation, the filtered incompressible Navier-Stokes equations can be expressed as:

$$\frac{\partial \bar{u}_i}{\partial x_i} = 0 \qquad (1$$

$$\frac{\partial \bar{u}_i}{\partial t} + \frac{\partial \bar{u}_i \bar{u}_j}{\partial x_j} = -\frac{1}{\rho}\frac{\partial \bar{p}}{\partial x_i} + \frac{\partial}{\partial x_j}\left[2\upsilon \bar{S}_{ij}\right] - \frac{\partial \tau_{ij}}{\partial x_j} - g_i[1 - \beta(\bar{T} - T_0)] \qquad (2$$

$$\frac{\partial \bar{T}}{\partial t} + \frac{\partial \bar{u}_j \bar{T}}{\partial x_j} = \frac{\partial}{\partial x_j}\left[\alpha \frac{\partial \bar{T}}{\partial x_j}\right] - \frac{\partial \tau_{jT}}{\partial x_j} \qquad (3$$

Where the $\bar{\Delta} = \sqrt[3]{\Delta x \Delta y \Delta z}$ was chosen as the effective filter width. x_i denotes the i^{th} coordinate direction. $\bar{u}_i$ represents the filtered velocity field in the x_i direction, t the time, $\bar{p}$ the modified filtered pressure, and $\bar{T}$ the filtered temperature. The last term in Equation (2) is the buoyancy term where β is thermal expansion of the fluid and g_i the gravitational acceleration. The parameters υ, α

indicate the kinematic viscosity and thermal diffusivity, respectively. The subgrid scale (SGS) stress tensor and the scalar SGS thermal flux vector is included, respectively, in the momentum and energy equations above via the unresolved terms $\tau_{ij} = \overline{u_i u_j} - \bar{u}_i \bar{u}_j$ and $\tau_{jT} = \overline{u_j T} - \bar{u}_j \bar{T}$.

Modeling of unresolved turbulent scales

The closure of the Navier–Stokes equations can be achieved by utilizing the Wall-Adapting Local Eddy-viscosity (WALE) turbulence model for calculating the SGS kinematic viscosity, υ_{SGS}, based on the invariants of the velocity gradient tensor;

$$\tau_{ij} = \overline{u_i u_j} - \bar{u}_i \bar{u}_j = -2\upsilon_{SGS}\bar{S}_{ij} + \frac{2}{3}k_{SGS}\delta_{ij} \qquad (4$$

$$\upsilon_{SGS} = \bar{\Delta}^2 C_w^2 \frac{\left(\bar{S}_{ij}^* \bar{S}_{ij}^*\right)^{3/2}}{\left(\bar{S}_{ij}\bar{S}_{ij}\right)^{5/2} + \left(\bar{S}_{ij}^* \bar{S}_{ij}^*\right)^{5/4}} \qquad (5$$

$$\bar{S}_{ij}^* = \frac{1}{2}\left(\bar{g}_{ij}^2 + \bar{g}_{ji}^2\right) - \frac{1}{3}\bar{g}_{kk}^2\delta_{ij} \qquad (6$$

$$\bar{g}_{ij}^2 = \bar{g}_{ik}\bar{g}_{kj} = \frac{\partial \bar{u}_i}{\partial x_k}\frac{\partial \bar{u}_k}{\partial x_j} \qquad (7$$

Where C_w is the model coefficient, here taken at a constant value equal to 0.325 [11]. k_{SGS} and $\bar{S}_{ij}$ are the SGS kinetic energy and resolved scale strain rate tensor.

$$\bar{S}_{ij} = \frac{1}{2}\left(\frac{\partial \bar{u}_i}{\partial x_j} + \frac{\partial \bar{u}_j}{\partial x_i}\right) \qquad (8$$

By analogy to the SGS stress tensor modeling, the scalar SGS thermal flux vector, τ_{jT}, can be approximated by the following expression [12];

$$\tau_{jT} = \overline{u_j T} - \bar{u}_j \bar{T} = -\frac{\upsilon_{SGS}}{Pr_{SGS}}\frac{\partial \bar{T}}{\partial x_j} \qquad (9$$

Where Pr_{SGS} denotes the SGS Prandtl number and is fixed at 0.85 in the simulations presented below. The WALE turbulence model is able to reproduce the near-wall behavior correctly. Thus, opposed to most eddy viscosity turbulence models that require wall-damping functions near the wall region, the turbulent viscosity obtained by WALE formulation approaches zero at the wall. The model also generates zero turbulent viscosity in case of a pure shear; hence it can capture the transitional flow from laminar to turbulent [13].

Computational grid and boundary conditions

To achieve high resolution using minimum number of mesh elements, the mesh has been refined in four zones with different grid sizes. The finest elements of the structured mesh concentrates predominantly in a region around the middle of the door to properly resolve 3-D interfacial mixing, re-entrainment phenomena, and other fluctuation structures. An unstructured mesh with a combination of tetrahedra and pyramid cells was employed in the other three refinement zones. A smooth transition between the cell of different sizes is performed. In total, nearly 25 million elements have been spread all over the multizone enclosure. The computational grid is shown in Fig. 3.

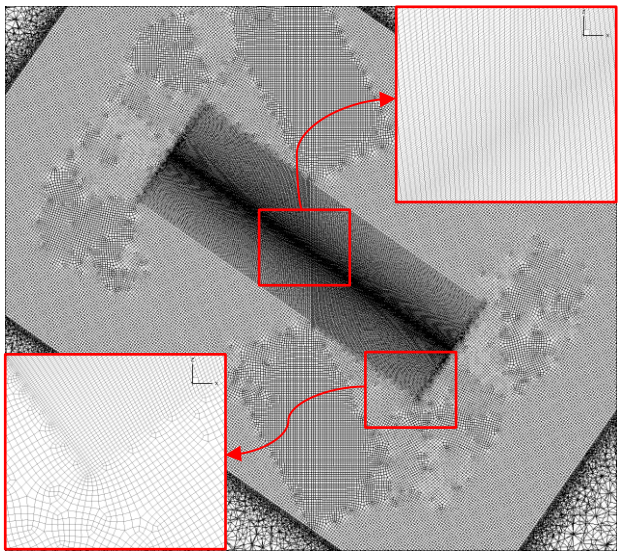

Figure 3: Computational grid.

Uniform initial temperature of $T_c = 293.15K$ and $T_H = 298.15K$ is imposed in the cold and warm reservoirs, respectively $(\Delta T = 5K)$. The reference temperature (T_{ref}) is the arithmetic average of these two temperatures. The Prandtl number, $Pr = 0.73$, kinematic viscosity, $\upsilon = 1.538 \times 10^{-5}\, m^2/s$, and thermal expansion coefficient of the air, $\beta = 1/T_{ref} = 0.00335$, were applied. The enclosure is initialized with zero velocity, which would guarantee that natural convection would evolve. External walls of the enclosure are adiabatic and with a no-slip boundary condition.

During the first step of the simulation, an adaptive time step has been considered until the start-up fluctuations disappeared. Afterward, a constant time step of $\Delta t = 0.01$ is maintained to keep the Courant number value below 1.0 in order to achieve temporal accuracy and numerical stability. Note that a pseudo-stationary condition is reached after about 60 seconds when the airflow has fully established throughout the enclosure and the transition to turbulent mixing is settled. In this pseudo-steady state regime, the statistical data of time-averaged flow variables is collected for 80 seconds in order to reach full-converged statistics. During this period, the volume-averaged air temperature of both reservoirs remains almost constant.

Numerical Methodology

The non-linear governing equations are discretized using the second-order cell-centered finite volume method (FVM) implemented in the ANSYS Fluent commercial CFD package. The algorithm of Semi-Implicit Method for Pressure Linked Equations (SIMPLE) is employed for decoupling of velocity and pressure in the Navier–Stokes equations. The time derivatives are advanced in time using the Second Order Implicit scheme. The Bounded Central Differencing scheme is adopted for the treatment

of the convective term in the momentum equation. The diffusion terms are central-differenced, while the pressure interpolation is provided by the Body Force Weighted scheme.

ANSYS Fluent is capable of running on distributed processors and uses the public domain openMPI implementation of the standard message passing interface (MPI) to conduct inter-processor communication. The present LES simulation was carried out on the Idun cluster [14], containing Intel Xeon processor nodes with 40 cores and a minimum of 128GB of RAM.

Results and discussion

Interfacial Mixing

The counterflowing streams start setting up once the aperture opens and creates an opening between cold and warm zones. As expected, both warm and cold airflows are initially laminar and after a few seconds, they become turbulent. The low-density warm air descends in the heated plate side of the partition wall and is discharged into the adjacent cold zone by bending rapidly over the upper part of the opening and rise as a buoyant plume due to Archimedes force. Since the dimensions of the two reservoirs are considerable compared to the aperture area, temperature changes in each reservoir will be negligible.

Both air streams will meet at some distance from the bottom and up edges of the opening, where this interface is called the neutral plane. At the position of the neutral plane, the velocity would be zero and the pressure in both rooms are equal; hence there will be no airflow. When the flow is inviscid, there is no mixing or heat transfer between the two opposite airstreams close to and within the aperture. With viscous effects, instantaneous results provided by LES in Fig. 4 show unsteady flow structures developing in the middle of the doorway.

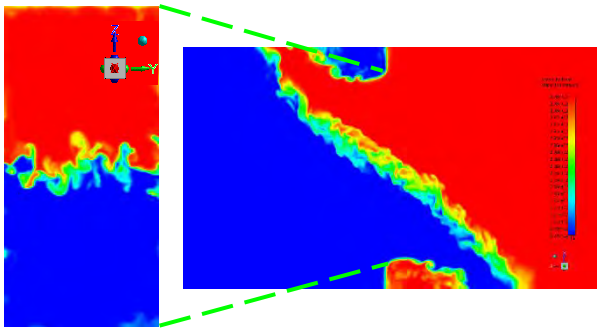

Figure 4: Instantaneous temperature in the door (left) and in a lateral view at the middle of the door in the y-direction (right).

The neutral plane (NP) is clearly visible in the left figure which shows front views of the door. This plane is not straight, and its position fluctuates slightly in space and time. To the authors' best knowledge, this effect has never been reported in the literature. The flow can also be visualized in a plane perpendicular to the door (right figure).

A snapshot of the mean temperature contours on a vertical plane in the middle of the enclosure are presented in Fig. 5. The counterflow develops from the NP with an angle of approximately 35 degrees with the horizontal. Unlike the standard theory assuming the flow to be horizontal at the doorway level, the CFD is strongly three-dimensional. Compared to inviscid flow (i.e. Euler simulation), the interfacial mixing induces a smoother transition of the temperature between both airstreams for viscous flow.

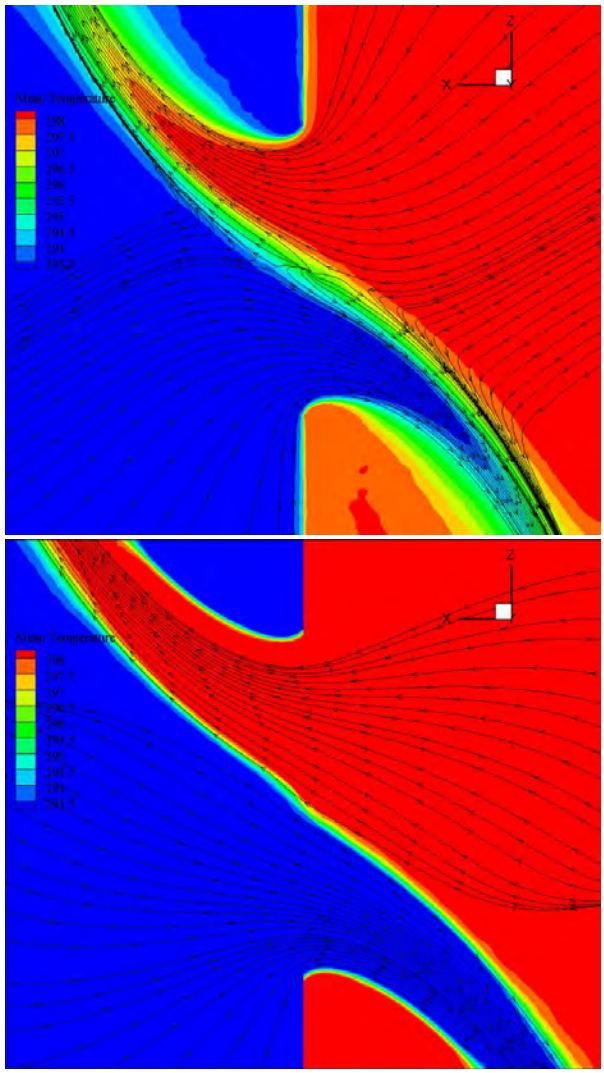

Figure 5: Mean temperature contours with streamlines, (LES above and Euler below).

The streamlines in viscous flow reveal that interfacial mixing causes a fraction of the warm airflow to be brought back into the warm zone, entrained by the cold airstream. This re-entrainment is similar for the cold airflow. However, no re-entrainment happened when the viscosity is switched off (Euler). The sharp edges of the aperture cause flow separation. At a section slightly downstream of the opening where the streamlines get almost horizontal, the maximum flow contraction takes place. In this section, the effective cross-section area for the airflow passage is minimum leading to the maximum velocity magnitude. This narrowest flow region is known as *vena contracta* and can occur when streamlines are unable to

follow sharp angles of openings. This area is shown by the streamlines passing through the aperture in Fig. 5, while it is not predicted by the theoretical model. The contraction will affect the airflow rate (or C_d) and heat exchange through the aperture.

Profiles of the time-averaged streamwise velocity and air temperature along a line in the middle of the doorway are shown in Fig. 6. The simulation results are also compared with those obtained by Euler simulation. For the theory, the velocity is scaled by a C_d calibrated by the LES (see next subsection). The first figure shows that the streamwise velocity is very similar between the LES, Euler simulation and the theory (denoted by Bernoulli) away from the middle of the door where the mixing takes place. The theory is able to successfully reproduce the streamwise velocity over a large part of the doorway. This can explain why this theory has been widely used in practice when an estimate of C_d is available. In the middle of the doorway, the Euler simulation and the theory also show similar results.

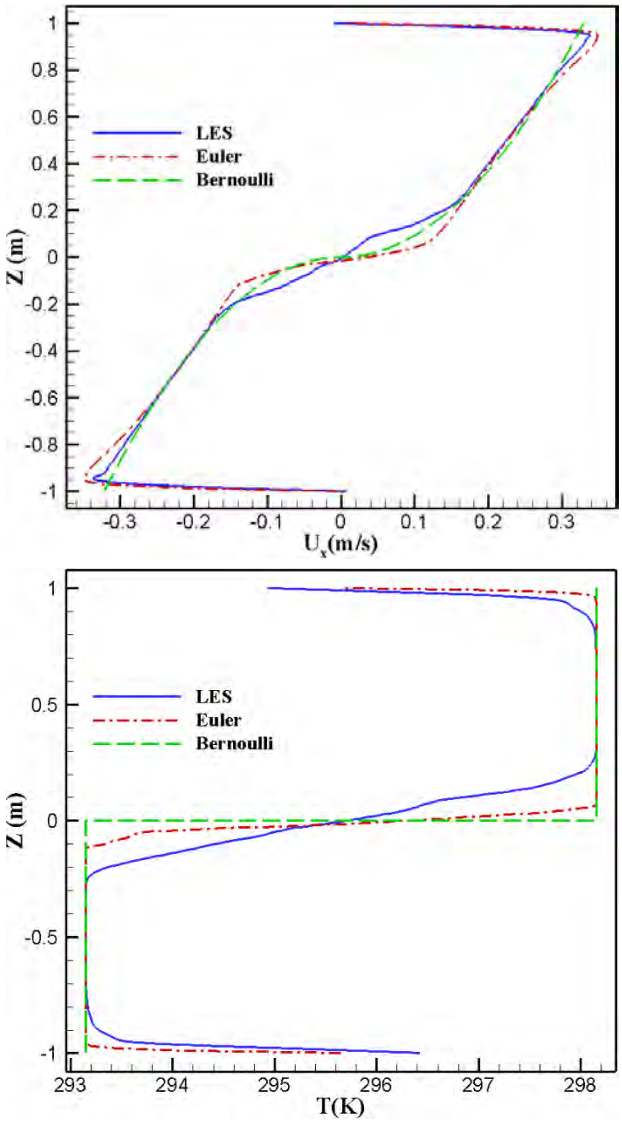

Figure 6: Time-averaged streamwise velocity and temperature profiles in the middle of the doorway.

It is only by introducing viscous effects and the resulting mixing that the velocity field shows a smoother transition. This transition zone has a length of 0.2 H, centered on the NP.

The mean temperature profiles confirm these conclusions. The LES and Euler simulation give similar results over a large fraction of the door. In the middle of the doorway, the Euler temperature profile is close to a step function of 5K as assumed by the theory. On the contrary, the LES has a smoother transition.

Bulk Quantities

Considering the Bernoulli equation for an inviscid horizontal airflow passing through the aperture, the maximum theoretical volume flow rate (Q_{max}) can be evaluated as [9]:

$$Q_{max} = \frac{A}{3}\sqrt{g' H} \qquad (10)$$

$$g' = g\frac{\Delta\rho}{\rho_e} \qquad (11)$$

$$\rho_e = \rho_w \frac{\left(1 + (\rho_c/\rho_w)^{1/3}\right)^3}{8} \qquad (12)$$

$$Q = C_d Q_{max} \qquad (13)$$

Where A and H are the aperture area and height, respectively. g' is defined as the effective acceleration of gravity. For low temperature differences until $40K$ the effective density, ρ_e, can be replaced with the average density [9]. The value of C_d is computed by dividing the actual volume flow rate (Q) by the maximum theoretical volume flow rate from the theory (Q_{max}). The time histories of the total volume flow rate, volume flow rate of each air stream, heat transfer, and doorway orifice coefficient are shown in Fig. 7.

The total volume flow rate of the warm and cold airflows respects the conservation of mass. In other words, the mass flow entering the sealing room must equal the mass flow leaving the room. As both reservoirs are adiabatic, energy is also conserved and the convective heat flow (Qc) of both airstreams has the same magnitude but opposite signs.

Besides the existence of small fluctuations in Fig 4., LES and Euler approaches produce nearly the same values of each bulk quantity (i.e. volume flow rate, C_d and heat transfer). Hence it can be concluded that bulk quantities will not be affected significantly by unsteady flow structures developing along the counterflow interface.

Conclusions

The characteristics of the three-dimensional bulk flow through a large vertical opening induced by the temperature difference of two isothermal reservoirs have been extensively studied in the literature. However, factors influencing the flow (or the discharge coefficient, C_d), such as unsteady flow phenomena should still be studied. ANSYS Fluent was used to investigate this effect. LES using the WALE subgrid scale model was

adopted to predict the unsteady turbulent behaviour of the counterflowing airstreams. Results were compared to

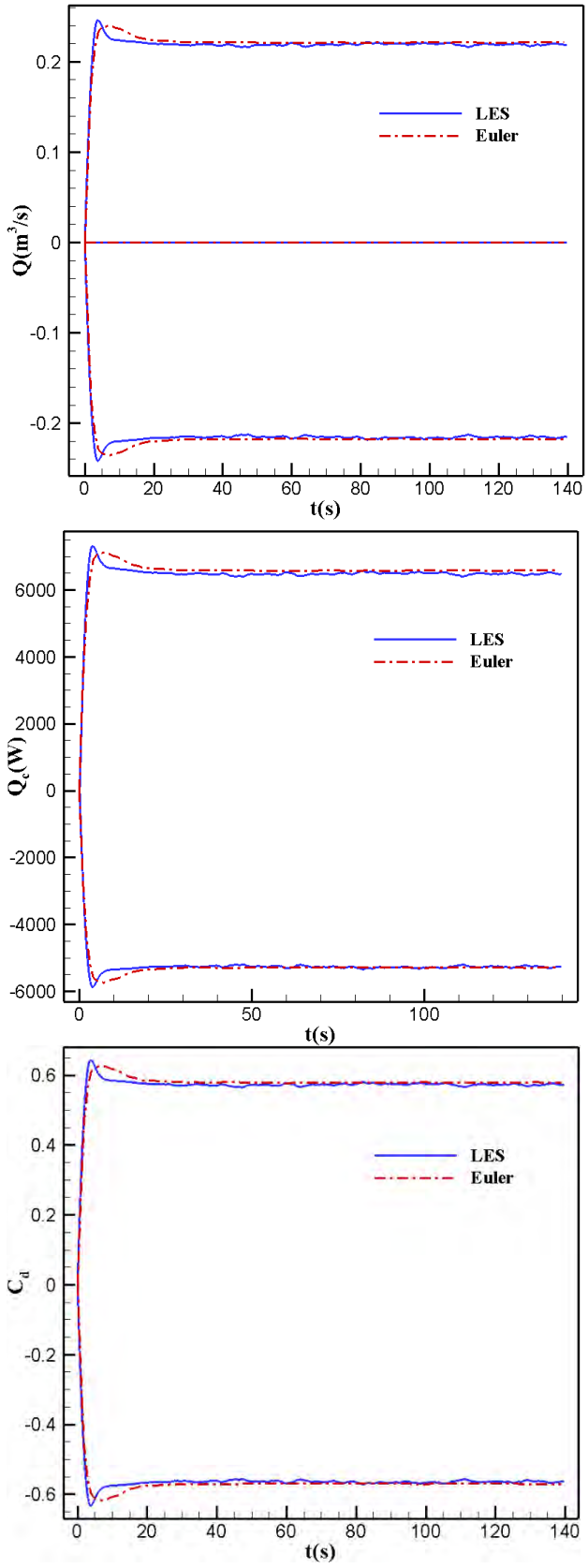

Figure 7: Time histories of mass flow rate, heat transfer, and doorway orifice coefficient.

Euler simulation. The inviscid flow showed no mixing or heat transfer between the opposite airflows close to and within the aperture. On the contrary, unsteady flow structures near the neutral plane were predicted by LES and generate interfacial mixing. Three phenomena resulted from the two counterflowing warm and cold airstreams (i.e. shear layer, re-entrainment effects and unsteady flow structures) and led to a reduction of the mass flow and heat exchange through the doorway. The theory was able to fairly reproduce the streamwise velocity and air temperature over a large fraction of the doorway. However, significant differences between viscous (i.e. LES) and inviscid flows (i.e. Euler and theoretical model) were present in the middle of the doorway ($|z| < 0.2$ H) due to mixing. Even though unsteady flow structures were present in the middle of the doorway, bulk quantities such as C_d were not affected significantly. The values of C_d calibrated by the LES and Euler simulation were very similar.

References

[1] D. Scott, R. Anderson, and R. Figliola, "Blockage of natural convection boundary layer flow in a multizone enclosure," *International journal of heat and fluid flow,* vol. 9, no. 2, pp. 208-214, 1988.

[2] J. Neymark, C. R. Boardman III, A. Kirkpatrick, and R. Anderson, "High Rayleigh number natural convection in partially divided air and water filled enclosures," *International Journal of Heat and Mass Transfer,* vol. 32, no. 9, pp. 1671-1679, 1989.

[3] L. Georges, G. Cao, and H. M. Mathisen, "Further Investigation of the Convective Heat Transfer between Rooms through Open Doorways," in *the 12th REHVA World Congress: volume 5. Aalborg: Aalborg University, Department of Civil Engineering.*, 2016.

[4] P. Favarolo and H. Manz, "Temperature-driven single-sided ventilation through a large rectangular opening," *Building and Environment,* vol. 40, no. 5, pp. 689-699, 2005.

[5] D. Agonafer, L. Gan-Li, and D. B. Spalding, "The LVEL turbulence model for conjugate heat transfer at low Reynolds numbers," *Application of CAE/CAD Electronic Systems, ASME,* vol. 18, pp. 23-26, 1996.

[6] F. Allard and Y. Utsumi, "Airflow through large openings," *Energy and Buildings,* vol. 18, no. 2, pp. 133-145, 1992.

[7] R. Pelletret, G. Liebecq, F. Allard, J. Van der Maas, and F. Haghighat, "Modelling of large openings," in *12th AIVC Conference: Air Movement and Ventilation Control Within Buildings*, 1991.

[8] F. Allard *et al.*, "Airflow through large openings in buildings," *Annex 20: Air flow patterns within Buildings,* 1992.

[9] D. Wilson and D. Kiel, "Gravity driven counterflow through an open door in a sealed room," *Building and Environment,* vol. 25, no. 4, pp. 379-388, 1990.

[10] A. Lefauve, J. Partridge, and P. Linden, "Regime transitions and energetics of sustained stratified shear

flows," *Journal of Fluid Mechanics,* vol. 875, pp. 657-698, 2019.
[11] F. Nicoud and F. Ducros, "Subgrid-scale stress modelling based on the square of the velocity gradient tensor," *Flow, turbulence and Combustion,* vol. 62, no. 3, pp. 183-200, 1999.
[12] A. Leonard, "Energy cascade in large-eddy simulations of turbulent fluid flows," *Adv. Geophys. A,* vol. 18, no. A, pp. 237-248, 1974.
[13] A. Yuen, G. Yeoh, V. Timchenko, S. Cheung, and T. Chen, "Study of three LES subgrid-scale turbulence models for predictions of heat and mass transfer in large-scale compartment fires," *Numerical Heat Transfer, Part A: Applications,* vol. 69, no. 11, pp. 1223-1241, 2016.
[14] M. Själander, M. Jahre, G. Tufte, and N. Reissmann, "EPIC: An energy-efficient, high-performance GPGPU computing research infrastructure," *arXiv preprint arXiv:1912.05848,* 2019.